ARMY RESEARCH LABORATORY

A Technique for Calibrating the Phase Detector of a Wideband Radar Using an External Target

by
H. Bruce Wallace and Thomas J. Pizzillo

ARL-TR-1521 March 1998

The findings in this report are not to be construed as an official Department of the Army position unless so designated by other authorized documents.

Citation of manufacturer's or trade names does not constitute an official endorsement or approval of the use thereof.

Destroy this report when it is no longer needed. Do not return it to the originator.

Army Research Laboratory
Adelphi, MD 20783-1197

ARL-TR-1521 **March 1998**

A Technique for Calibrating the Phase Detector of a Wideband Radar Using an External Target

H. Bruce Wallace and Thomas J. Pizzillo
Sensors and Electronic Devices Directorate

Abstract

A signal processing method is presented for correcting imbalances in the phase-detection channels of a coherent, wideband radar. The technique, an expansion of an earlier method, derives phase and gain corrections using an external point target illuminated by a wideband waveform. The technique does not depend upon the target or the phase and gain flatness of the radar waveform. Errors remaining after application of this technique depend on the signal-to-noise ratio and the correlation of the sampling with the radar waveform.

Contents

Figures

1. Introduction

Inverse synthetic aperture radars (ISARs) transmit a wideband waveform to derive range information. Most systems use a linear or stepped frequency modulated waveform, generated either analog or digitally, that may be processed with a fast Fourier transform (FFT) to produce a high-resolution range profile.[1] To obtain such a profile, the system must relate the returned signal measured by the radar to the transmitted signal or to an internal reference signal in a known fashion. While this comparison may be made in a wideband phase-comparison receiver, we concentrate here on using a narrow-band phase-detector system. In this class of system, the received signal is down-converted into a narrow bandwidth by the received, coherent signal being separated into two channels, which are then mixed with two orthogonal local oscillator (LO) signals. Typically, calibration techniques for these systems determine the individual error sources through a series of internal and external means; this report describes a technique that uses only an external point target. This technique is an improvement of the method presented by Churchill et al,[2] in that calibration may be obtained from an external target of opportunity, eliminating the need for internal calibration hardware.

For this work, we developed a signal model based on certain assumptions that we present here. This model is the basis for our technique for deriving the correction coefficients, which we describe along with its limitations. We identify two error sources associated with this calibration technique, and discuss how to prevent these errors. Finally, we conclude that our method offers improved performance over the earlier method,[2] in terms of practical considerations not discussed by Churchill et al.[2]

2. Derivation of Correction Coefficients

2.1 Description of Calibration Technique

Figure 1 is a diagram of the phase-detector system, showing the following inputs/outputs: the received, intermediate frequency (IF) signal, the LO, and the resultant in-phase (I) and quadrature phase (Q) signals. The resultant signals I and Q define the real and imaginary parts of the received signal before digitization.

This portrayal of the detection process suggests that the signal received is modified only by the target of interest. In reality, the signal is modified by the radar on transmission and reception, because of imperfections in the system's components. Figure 1 includes circuit elements representing these imperfections, including the following.

[1] *D. L. Mensa, High Resolution Radar Cross-Section Imaging, Artech House (1991), chapter 4.*

[2] *F. E. Churchill, G. W. Ogar, and B. J. Thompson, "The correction of I and Q errors in a coherent processor," IEEE Trans. Aerosp. Electron. Syst.* ***AES-17****, 131–137 (January 1981).*

- The 90° hybrid may actually shift the LO 90° ± δ°, where δ is a differential phase.
- The mixers have dc offsets represented as a voltage source referenced to ground.
- The gain throughout the phase-detector system is different for the *I* and *Q* channels; these different gains are represented by G_i and G_q.

For simplicity, the gain and phase imperfections are represented as occurring in the *Q* channel only, which results in no loss in generality.

If the radar and phase detector were perfect, the measured outputs from the *I* and *Q* channels (for a point target) would be represented by two $1 \times N$ row vectors,

$$\mathbf{I}\left(f_N\right) = \left[A\cos\left(\phi\left(f_1\right)\right) \ldots A\cos\left(\phi\left(f_n\right)\right) \ldots A\cos\left(\phi\left(f_N\right)\right)\right], \quad (1)$$

$$\mathbf{Q}\left(f_N\right) = \left[A\sin\left(\phi\left(f_1\right)\right) \ldots A\sin\left(\phi\left(f_n\right)\right) \ldots A\sin\left(\phi\left(f_N\right)\right)\right],$$

where $f = [f_1 \ldots f_n \ldots f_N]$ represents the N frequency steps of a pulse-compression system, $\phi(f_n)$ represents the relative phase between the *I* and *Q* channels (which is linearly dependent on frequency), N is the number of frequency steps in the pulsed stepped waveform, and A is the amplitude of the received signal. Equations (1) describe the ideal form of the received signal that we would like to measure. However, the measured signal is that signal actually produced by the radar phase detector and includes the effects of each of the imperfections diagrammed in figure 1.

In addition to these errors, there are corruptions due to imperfections in the transmitted waveform and in the wideband receiver, and there are effects due to targets that are not purely point-like. Because these imperfections are introduced before the signal reaches the phase detector, each channel is affected equally in both amplitude and phase, and the imperfec-

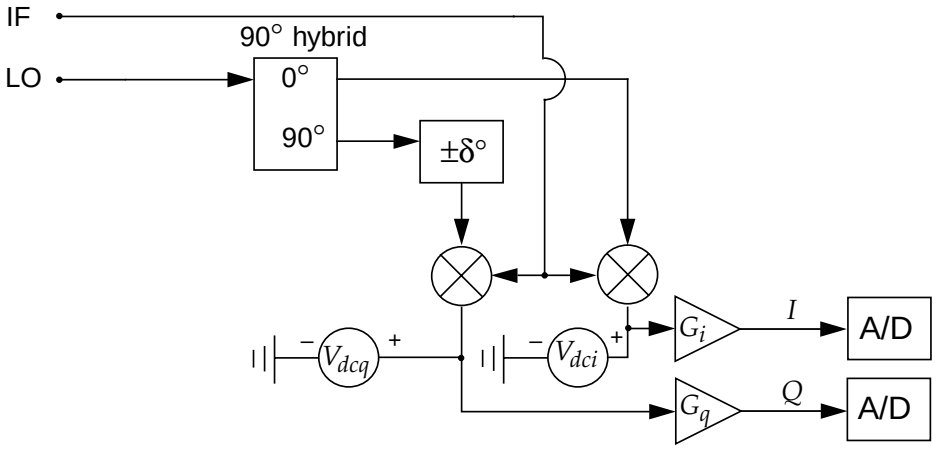

Figure 1. Generalized narrow-band phase-detector system.

tions are resolved by other radar calibration processing steps not addressed in this report.

In a real, imperfect radar and phase detector, the imperfections in figure 1 would result in a measured signal containing errors. The effect of these errors on the nth element of the $1 \times N$ row vectors of equation (1) is represented by

$$\begin{aligned} \mathbf{I}_m(f_n) &= A\cos\left(\phi(f_n)\right) + V_{dci} \quad , \\ \mathbf{Q}_m(f_n) &= GA\sin\left(\phi(f_n) + \delta\right) + V_{dcq} \quad , \end{aligned} \tag{2}$$

where $\mathbf{I}_m(f_n)$ and $\mathbf{Q}_m(f_n)$ are the measured I and Q signals of the nth frequency step of the pulse, G represents the gain imbalance in the phase-detector channels (assumed to be positive and real), δ represents the phase imbalance introduced by the imperfect 90° hybrid, and V_{dci} and V_{dcq} are the dc offsets in each channel. If we assume that the target of opportunity from which we would like to measure our calibration is a point target, we need only one measurement to correct for all errors except for dc components. This assumption is reasonable provided our target falls within one range cell. By algebraic manipulation of equations (2), we can represent the elements of equations (1) in terms of measured and derived parameters:

$$\begin{aligned} \mathbf{I}(f_n) &= \mathbf{I}_m(f_n) - V_{dci} \quad , \\ \mathbf{Q}(f_n) &= \frac{\mathbf{Q}_m(f_n) - V_{dcq}}{G\cos\delta} - \mathbf{I}(f_n)\tan\delta \quad . \end{aligned} \tag{3}$$

V_{dci} and V_{dcq} are the means of each channel and may be determined directly.

Now only the values G and δ require determination; our proposed process determines the best values for these variables. Best values are defined as those values that scale and orthogonalize $\mathbf{Q}_m(f_N)$ and $\mathbf{I}_m(f_N)$. When $\mathbf{Q}_m(f_N)$ and $\mathbf{I}_m(f_N)$ are orthogonal, the FFT of a point target has a single peak at the appropriate range bin and no output at the image range bin.[3] Hence, a technique for making equations (2) orthogonal uses the FFT as a narrowband filter. Because we are using signals from point sources, the range bin of the peak value of the FFT of the $\mathbf{Q}_m(f_N)$ and $\mathbf{I}_m(f_N)$ is used to determine the correction factors. The coefficient of the peak-magnitude value of the FFT is a complex number that represents the amplitude and phase of the signal, passed through the narrow bandpass of the range bin in which it is found. If both the I and Q values are passed through the same bandpass filter separately, we can directly compare the gain and phase to determine the appropriate correction factors. (Note that if the frequency corresponding to the target response is known a priori, an FFT is not required, since the Churchill et al method[2] would suffice.)

[2] *F. E. Churchill, G. W. Ogar, and B. J. Thompson, "The correction of I and Q errors in a coherent processor," IEEE Trans. Aerosp. Electron. Syst.* ***AES-17****, 131–137 (January 1981).*

[3] *Merril Skolnik, Radar Handbook, 2nd edition, McGraw-Hill Inc. (1990), p 3.41.*

To determine the gain and phase imbalances G and δ, we must find the location of the peak magnitude in the complex FFT of the $\mathbf{Q}_m(f_N)$ and $\mathbf{I}_m(f_N)$ data. This first FFT is used to identify the location of the true response (as already noted, the true response is larger than the image response). We then compute complex FFT's of the I and Q vectors individually; that is, we form the complex vectors $(\mathbf{I}_m(f_N),0)$ and $(\mathbf{Q}_m(f_N),0)$ to determine the amplitudes and phases of the coefficients at the true-response frequency. These are given by

$$F\left[\left(\mathbf{I}_m(f),0\right)\right] = \sum_{n=0}^{N-1} A\cos\left(\phi(f_n)\right)\exp\left(\frac{j2\pi kn}{N}\right) = I(k) \quad , \tag{4}$$

$$F\left[\left(\mathbf{Q}_m(f),0\right)\right] = \sum_{n=0}^{N-1} GA\sin\left(\phi(f_n)+\delta\right)\exp\left(\frac{j2\pi kn}{N}\right) = Q(k) \quad , \tag{5}$$

where $I(k)$ and $Q(k)$ are the K complex outputs of the FFT, $K = 1 \ldots k \ldots N$.

The results of equations (4) and (5) provide the location of the peak responses, $Q(k)\big|_{\max}$ and $I(k)\big|_{\max}$, where k is the kth range cell, r_k, of the range profile:

$$Q(k)\Big|_{peak} = AG\left[\cos\left(r_k+\delta\right)+j\sin\left(r_k+\delta\right)\right] = AGe^{j(r_k+\delta)} \quad , \tag{6}$$

$$I(k)\Big|_{peak} = A\left[\cos\left(r_k\right)+j\sin\left(r_k\right)\right] = Ae^{j(r_k)} \quad . \tag{7}$$

The gain imbalance is related to the ratio of the power P_i and P_q, at this location, since

$$\frac{Q(k)}{I(k)} = G\,(\cos\delta + j\sin\delta) \tag{8}$$

so that

$$\frac{P_q}{P_i} = \left(\frac{\left|Q(k)\right|}{\left|I(k)\right|}\right)^2 = G^2 \quad . \tag{9}$$

Therefore,

$$G = \sqrt{\frac{P_q}{P_i}} \quad . \tag{10}$$

The phase correction is found through the use of the following unambiguous trigonometric identity (π is added to shift the range of values from the principal branch to $0 - 2\pi$):

$$\delta = \pi + 2\arctan\left(\frac{\sin\delta}{1+\cos\delta}\right) \quad . \tag{11}$$

By substituting the real and imaginary parts of equation (8), we get

$$\delta = \pi + 2 \arctan\left(\frac{\mathrm{Im}\left(\frac{Q(k)}{I(k)}\right)}{G + \mathrm{Re}\left(\frac{Q(k)}{I(k)}\right)}\right) \quad . \tag{12}$$

Therefore, after the dc biases are removed from the I and Q signal components by subtraction of the associated averages, we need only three FFT's of a single data set taken from an arbitrary target to determine the phase and gain corrections: one FFT to locate the peak signal from the complex pair (I, Q), and two more to produce the correction factors—one each for the real (I, 0) and imaginary (Q, 0) correction factors.

One limitation to this technique is the possibility that the peak may occur at the center or either end of the FFT. In any of these positions, the image of the peak will be superposed with the peak, contaminating the gain and phase measurements. Additionally, the incremental phase change at these locations is zero, providing no information for calibration.

2.2 Example of Calibration Technique Using Simulated Data

We generated each of the plots in figures 2 to 8 from data to which a Hamming window was applied. Figure 2 shows simulated data from a point target that has a response centered in the 110th range cell of the range profile. The error values used in the model are as follows: V_{dci} = –0.9 V; V_{dcq} = 1.1 V; G = 1.5 V; δ = –3.5°; and signal to noise ratio (SNR) = 40 dB. Figure 3 shows the complex 512-point FFT of the simulated I and Q data, which is defined in equation (13). We generated these data using

Figure 2. Simulated I and Q response to a point target.

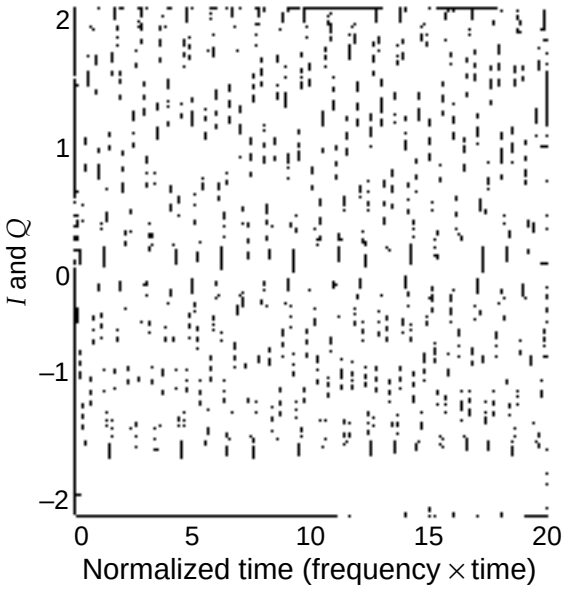

Figure 3. FFT of simulated *I* and *Q* response to a point target.

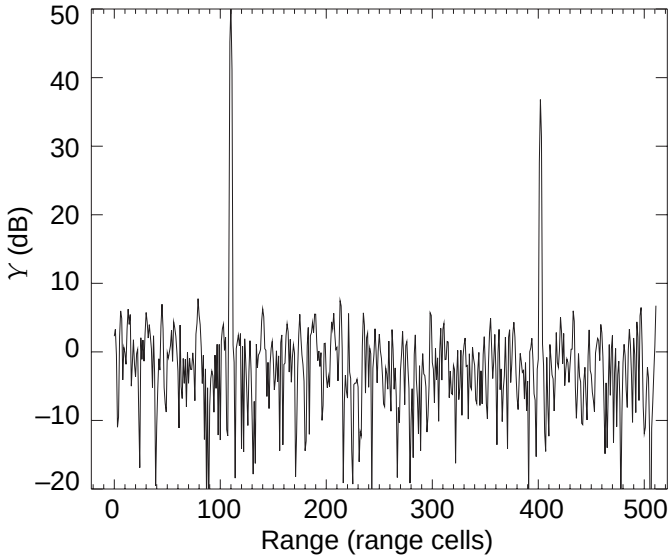

Figure 4. FFT of corrected *I* and *Q* response to a simulated point target.

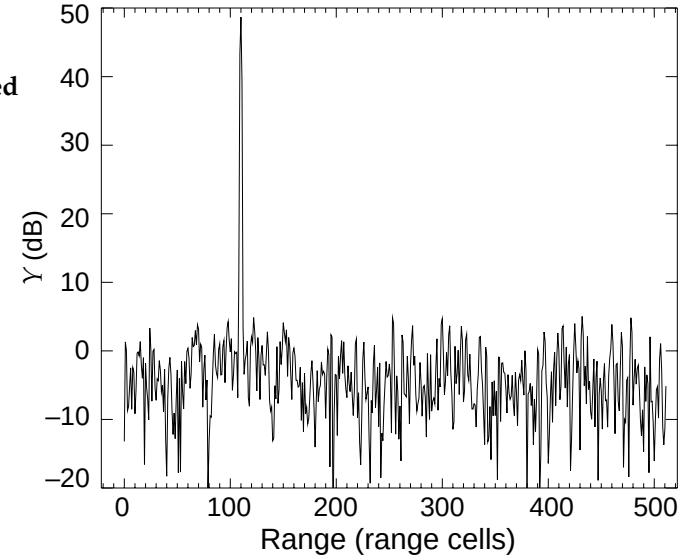

equation (2). In figures 3 and 4, the ordinate axis is the absolute value of the complex FFT of the measured data, represented by

$$Y = \left(\text{abs} \left[\text{cfft} \left\{ \left[\mathbf{I}_m (f_n) + i\mathbf{Q}_m (f_n) \right] + \mathbf{n}_g \right\} \right] \right) = \text{abs} \left[\text{cfft} \left\{ \mathbf{S}_m (f_n) \right\} \right] \quad \cdot \qquad (13)$$

Here, abs means "the absolute value of," cfft means "complex FFT," $\mathbf{n}_g$ represents a complex N-vector of white Gaussian noise, and S_m represents the entire measured signal.

To correct these data, we removed the dc offsets by subtracting the mean of the I and Q values, before correcting for the gain and phase imbalances, as described in the previous section. Figure 4 shows the complex FFT of the

corrected I and Q data. The correction factors, as determined by equations (10) and (12), are G = 1.501 V, δ = –3.56°, V_{dci} = –0.902 V, and V_{dcq} = 1.097 V. These are in good agreement with the values modeled.

2.3 Error Analysis

We generated figures 5 to 8 using a Monte Carlo simulation of 50 data sets. The correction factors for each data set were determined, and then the average value for each set of 50 correction factors was used to determine the error for each point on the plots.

Because our technique depends upon the FFT as a narrow bandpass filter, it is reasonable to expect the size of the FFT to affect the accuracy of the correction factors. Figures 5 and 6 are plots showing the dependence of the error in the predicted gain- and phase-correction factors, respectively, as a function of SNR for three FFT sizes: 128, 512, and 2048. The accuracy of the predicted values will also be affected if the peak response is not centered in a bin of the FFT; this factor, commonly referred to as scalloping loss, can be as great as 3.92 dB for data that are transformed with a rectangular window, while use of a Hamming window will reduce this loss to 1.78 dB.[4] Figures 7 and 8 show the dependence of the error in the predicted gain and phase correction factors as a function of the response passing through a single range cell for the three FFT sizes. The error introduced by these scalloping losses is reduced further by the I and Q signals being the same apparent frequency and, consequently, located in the same FFT bin. We can realize a further improvement by applying the Hamming window function to the data, and padding the result to a larger vector size before transforming.

Figure 5. Gain-correction error as a function of SNR.

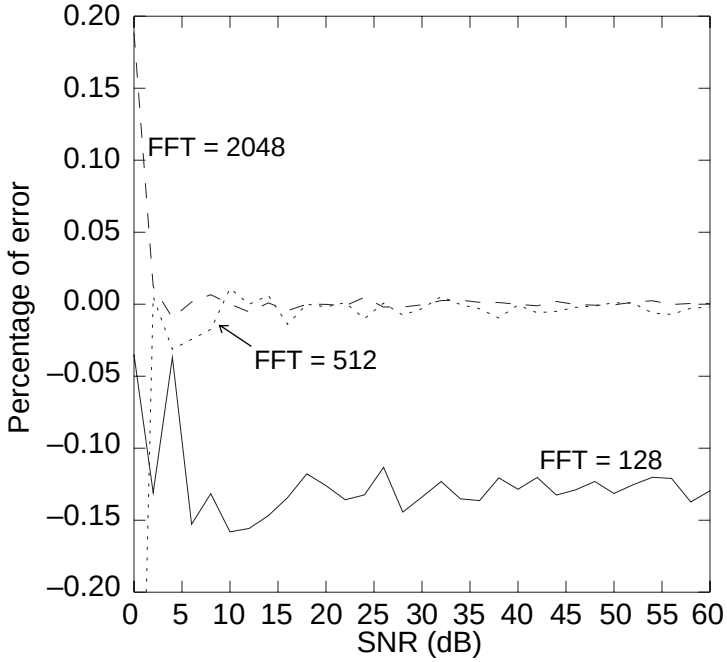

[4] *C. S. Lindquist, Adaptive and Digital Signal Processing with Digital Filtering Applications, vol. 2, Integrated Series in Signal Processing and Filtering, Stewart and Sons, Miami (1989), p 133.*

Figure 6. Phase-correction error as a function of SNR.

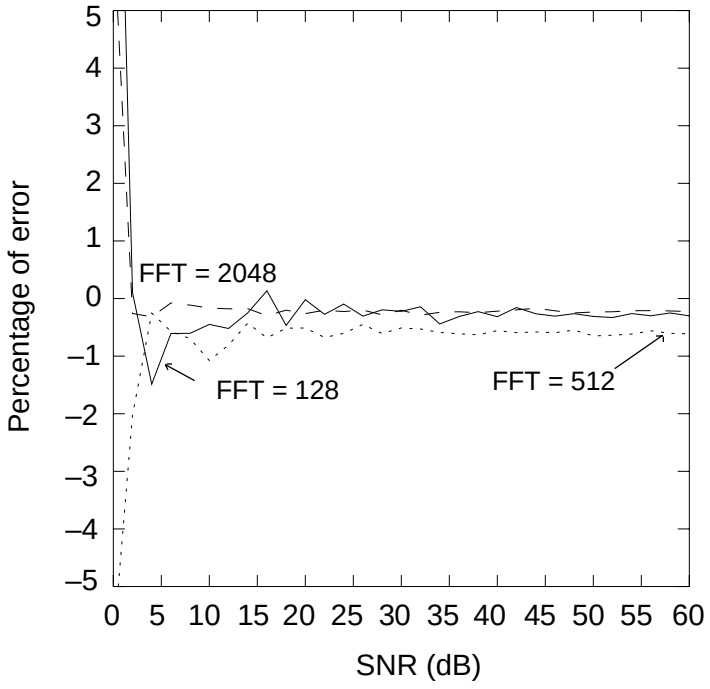

Figure 7. Gain-correction error as peak traverses one range cell.

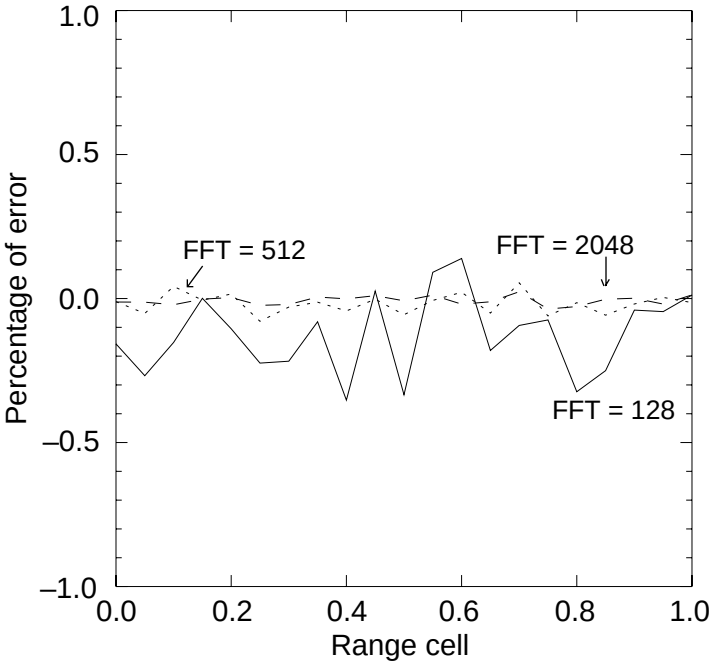

Figure 8. Phase-correction error as peak traverses one range cell.

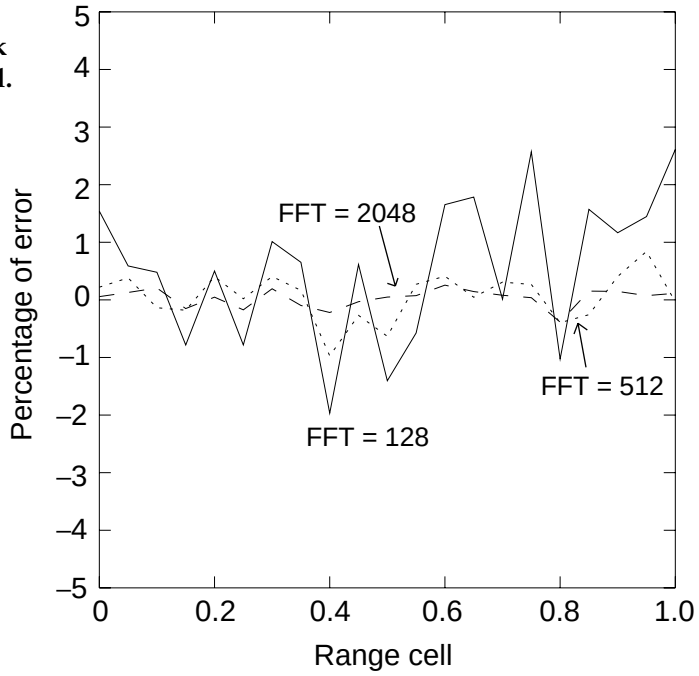

3. Conclusions

We present a method for correcting the I and Q imbalances of a wideband radar that requires no internal phase calibration hardware, and uses only data from an external target of opportunity (normally, an external target is required for absolute calibration of the system). The technique relies upon three FFT's of a single data set to determine gain- and phase-correction factors within an error that depends upon the signal-to-noise ratio of the data.

Distribution

Admnstr
Defns Techl Info Ctr
Attn DTIC-OCP
8725 John J Kingman Rd Ste 0944
FT Belvoir VA 22060-6218

Minister of Defense
Attn A Priou
Paris 22333
France

Ofc of the Dir Rsrch and Engrg
Attn R Menz
Pentagon Rm 3E1089
Washington DC 20301-3080

Ofc of the Secy of Defns
Attn ODDRE (R&AT) G Singley
Attn ODDRE (R&AT) S Gontarek
The Pentagon
Washington DC 20301-3080

OSD
Attn OUSD(A&T)/ODDDR&E(R) R Tru
Washington DC 20301-7100

Under Secy of Defns for Rsrch & Engrg
Attn Rsrch & Advncd Techlgy
Depart of Defns
Washington DC 20301

CECOM
Attn PM GPS COL S Young
FT Monmouth NJ 07703

CECOM NVESD
Attn AMSEL-RD-NV-ASD M Kelley
Attn AMSEL-RD-NV-TISD F Petito
FT Belvoir VA 22060

CECOM RDEC Elect System Div Dir
Attn J Niemela
FT Monmouth NJ 07703

CECOM
Sp & Terrestrial Commctn Div
Attn AMSEL-RD-ST-MC-M H Soicher
FT Monmouth NJ 07703-5203

Dpty Assist Secy for Rsrch & Techl
Attn SARD-TT F Milton Rm 3E479
The Pentagon
Washington DC 20301-0103

Hdqtrs Dept of the Army
Attn DAMO-FDT D Schmidt
400 Army Pentagon Rm 3C514
Washington DC 20301-0460

MICOM RDEC
Attn AMSMI-RD W C McCorkle
Redstone Arsenal AL 35898-5240

NGIC
Attn Iang RSC S Carter
Charlottesville VA 22902-5396

US Army Armament RDE Ctr
Attn SMCAR-FSP-A1 M Rosenbluth
Attn SMCAR-FSP-A1 R Collett
Picatinny Arsenal NJ 07806-5000

US Army CECOM NVESD
Attn AMSEL-RD-NV-RSPO A Tarbell
Attn AMSEL-RD-SR-R J Borowick
Mailstop 1112
FT Monmouth NJ 07703-5000

US Army CECOM Rsrch, Dev, & Engrg Ctr
Attn R F Giordano
FT Monmouth NJ 07703-5201

US Army Edgewood Rsrch, Dev, & Engrg Ctr
Attn SCBRD-TD J Vervier
Aberdeen Proving Ground MD 21010-5423

US Army Info Sys Engrg Cmnd
Attn ASQB-OTD F Jenia
FT Huachuca AZ 85613-5300

US Army Materiel Sys Analysis Agency
Attn AMXSY-D J McCarthy
Aberdeen Proving Ground MD 21005-5071

US Army Matl Command
Attn AMCDM Dir for Plans & Analysis
5001 Eisenhower Ave
Alexandria VA 22333-0001

Distribution (cont'd)

US Army Matl Cmnd
Dpty CG for RDE Hdqtrs
Attn AMCRD BG Beauchamp
5001 Eisenhower Ave
Alexandria VA 22333-0001

US Army Matl Cmnd
Prin Dpty for Acquisition Hdqrts
Attn AMCDCG-A D Adams
5001 Eisenhower Ave
Alexandria VA 22333-0001

US Army Matl Cmnd
Prin Dpty for Techlgy Hdqrts
Attn AMCDCG-T M Fisette
5001 Eisenhower Ave
Alexandria VA 22333-0001

US Army Missile Lab
Attn AMSMI-RD Advanced Sensors Dir
Attn AMSMI-RD Sys Simulation & Dev Dir
Attn AMSMI-RD-AS-MM G Emmons
Attn AMSMI-RD-AS-MM H Green
Attn AMSMI-RD-AS-MM M Christian
Attn AMSMI-RD-AS-MM M Mullins
Attn AMSMI-RD-AS-MM W Garner
Attn AMSMI-RD-AS-RPR Redstone Sci Info Ctr
Attn AMSMI-RD-AS-RPT Techl Info Div
Attn AMSMI-RD-SS-HW S Mobley
Redstone Arsenal AL 35809

US Army Natick Rsrch, Dev, & Engrg Ctr
Acting Techl Dir
Attn SSCNC-T P Brandler
Natick MA 01760-5002

US Army Rsrch Ofc
Attn G Iafrate
4300 S Miami Blvd
Research Triangle Park NC 27709

US Army Rsrch Ofc
Attn B D Guenther
Attn C Church
PO Box 12211
Research Triangle Park NC 27709-2211

US Army Simulation, Train, & Instrmntn Cmnd
Attn J Stahl
12350 Research Parkway
Orlando FL 32826-3726

US Army Tank-Automtv & Armaments Cmnd
Attn AMSTA-AR-TD C Spinelli
Bldg 1
Picatinny Arsenal NJ 07806-5000

US Army Tank-Automtv Cmnd
Rsrch, Dev, & Engrg Ctr
Attn AMSTA-TA J Chapin
Warren MI 48397-5000

US Army Test & Eval Cmnd
Attn R G Pollard III
Aberdeen Proving Ground MD 21005-5055

US Army Test & Eval Cmnd
Attn STEWS-TE-AF F Moreno
Attn STEWS-TE-LG S Dickerson
White Sands Missile Range NM 88002

US Army Train & Doctrine Cmnd
Battle Lab Integration & Techl Dirctrt
Attn ATCD-B J A Klevecz
FT Monroe VA 23651-5850

US Military Academy
Dept of Mathematical Sci
Attn MAJ D Engen
West Point NY 10996

USA CRREL
Attn G D Ashton
72 Lyme Rd
Hanover NH 03755

USA CRREL
Attn SWOE G Koenig
Attn SWOE P Welsh
72 Lyme Rd
Hanover NJ 03755

USAE Waterways Exprmnt Sta
Attn CEWES-EE-S J Curtis
Attn CEWES-EN-C W West
3909 Halls Ferry Rd
Vicksburg MS 39180-6199

Distribution (cont'd)

USATEC
Attn J N Rinker
Attn P Johnson
7701 Telegraph Rd
Alexandria VA 22315-3864

Nav Rsrch Lab
Attn 2600 Techl Info Div
4555 Overlook Ave SW
Washington DC 20375

Nav Surface Warfare Ctr
Attn Code B07 J Pennella
17320 Dahlgren Rd Bldg 1470 Rm 1101
Dahlgren VA 22448-5100

Nav Weapons Ctr
Attn 38 Rsrch Dept
Attn 381 Physics Div
China Lake CA 93555

AFMC Rome LAB/OC 1
Attn J Bruder
Griffiss AFB NY 13441-4314

Eglin Air Force Base
Attn 46 TW/TSWM B Parnell
211 W Eglin Blvd Ste 128
Eglin AFB FL 32542-5000

GPS Joint Prog Ofc Dir
Attn COL J Clay
2435 Vela Way Ste 1613
Los Angeles AFB CA 90245-5500

USAF Wright Lab
Attn WL/MMGS B Sundstrum
Attn WL/MMGS R Smith
101 W. Eglin Blvd Ste 287A
Eglin AFB FL 32542-6810

Sandia Natl Lab
PO Box 5800
Albuquerque NM 87185

DARPA
Attn B Kaspar
Attn L Stotts
Attn Techl Lib
701 N Fairfax Dr
Arlington VA 22203-1714

ARL Electromag Group
Attn Campus Mail Code F0250 A Tucker
University of Texas
Austin TX 78712

Eviron Rsrch Inst of MI
Attn C L Arnold
PO Box 134001
Ann Arbor MI 48113-4001

Georgia Inst of Techlgy
Georgia Tech Rsrch Inst
Attn Radar & Inrmntn Lab N C Currie
Attn Radar & Instrmntn Lab R McMillan
Attn Radar & Instrmntn Lab T L Lane
Atlanta GA 30332

Ohio State Univ Elect Sci Lab
Attn R J Marhefka
Columbus OH 43212

Univ of MichiganRadiation Lab
Attn F Ulaby
Attn K Sarabandi
3228 EECS Bldg 1301 Beal Ave
Ann Arbor MI 48109-2122

VA Polytechnic Inst & State Univ
Elect Interaction Lab
Attn G S Brown
Bradley Dept of Elect Engrg
Blacksburg VA 24061-0111

Dir for MANPRINT
Ofc of the Deputy Chief of Staff for Prsnnl
Attn J Hiller
The Pentagon Rm 2C733
Washington DC 20301-0300

Lockheed Martin Corp Elect & Missile Div
Attn E Weatherwax
5600 Sand Lake Rd Mail Stop 450
Orlando FL 32819

MIT Lincoln Lab
Attn E Austin
Attn W Keicher
PO Box 73
Lexington MA 02173-9108

Distribution (cont'd)

Simulation Technl
Attn A V Saylor
Attn D P Barr
PO Box 7009
Huntsville AL 35807

US Army Rsrch Lab
Attn AMSRL-P-S-E B Perlman
FT Monmouth NJ 07703-5601

US Army Rsrch Lab
Attn AMSRL-SE-RM B Bender
Attn AMSRL-SE-RM S Stratton
Attn AMSRL-WT-WB R A McGee
Aberdeen Proving Ground MD 21005

US Army Rsrch Lab
Attn AMSRL-CI-LL Techl Lib (3 copies)
Attn AMSRL-CS-AL-TA Mail & Records Mgmt
Attn AMSRL-CS-AL-TP Techl Pub (3 copies)
Attn AMSRL-SE J M Miller
Attn AMSRL-SE J Pellegrino

US Army Rsrch Lab (cont'd)
Attn AMSRL-SE-D E Scannell
Attn AMSRL-SE-EE Z G Sztankay
Attn AMSRL-SE-EO D Wilmot
Attn AMSRL-SE-RM B Wallace
Attn AMSRL-SE-RM C Ly
Attn AMSRL-SE-RM D Hutchins
Attn AMSRL-SE-RM D Wikner
Attn AMSRL-SE-RM E Burke
Attn AMSRL-SE-RM G Goldman
Attn AMSRL-SE-RM H Dropkin
Attn AMSRL-SE-RM J Nemarich
Attn AMSRL-SE-RM J Silverstein
Attn AMSRL-SE-RM J Silvious
Attn AMSRL-SE-RM P Cremona-Simmons
Attn AMSRL-SE-RM R Dahlstrom
Attn AMSRL-SE-RM R Wellman
Attn AMSRL-SE-RM T Pizzillo (20 copies)
Attn AMSRL-SE-RU B Scheiner
Attn AMSRL-SE-RU J Sichina
Adelphi MD 20783-1197

REPORT DOCUMENTATION PAGE

Form Approved
OMB No. 0704-0188

1. AGENCY USE ONLY *(Leave blank)*	2. REPORT DATE	3. REPORT TYPE AND DATES COVERED
	March 1998	Final, January 1997 to August 1997

4. TITLE AND SUBTITLE
A Technique for Calibrating the Phase Detector of a Wideband Radar Using an External Target

5. FUNDING NUMBERS
DA PR: AH16
PE: 62120A

6. AUTHOR(S)
H. Bruce Wallace and Thomas J. Pizzillo

7. PERFORMING ORGANIZATION NAME(S) AND ADDRESS(ES)
U.S. Army Research Laboratory
Attn: AMSRL-SE-RM
2800 Powder Mill Road
Adelphi, MD 20783-1197

8. PERFORMING ORGANIZATION REPORT NUMBER
ARL-TR-1521

9. SPONSORING/MONITORING AGENCY NAME(S) AND ADDRESS(ES)
U.S. Army Research Laboratory
2800 Powder Mill Road
Adelphi, MD 20783-1197

10. SPONSORING/MONITORING AGENCY REPORT NUMBER

11. SUPPLEMENTARY NOTES
AMS code: 622120.H16
ARL PR: 8NE4H2

12a. DISTRIBUTION/AVAILABILITY STATEMENT
Approved for public release; distribution unlimited.

12b. DISTRIBUTION CODE

13. ABSTRACT *(Maximum 200 words)*

A signal processing method is presented for correcting imbalances in the phase-detection channels of a coherent, wideband radar. The technique, an expansion of an earlier method, derives phase and gain corrections using an external point target illuminated by a wideband waveform. The technique does not depend upon the target or the phase and gain flatness of the radar waveform. Errors remaining after application of this technique depend on the signal-to-noise ratio and the correlation of the sampling with the radar waveform.

14. SUBJECT TERMS
ISAR, calibration, wideband radar, phase detector

15. NUMBER OF PAGES
20

16. PRICE CODE

17. SECURITY CLASSIFICATION OF REPORT	18. SECURITY CLASSIFICATION OF THIS PAGE	19. SECURITY CLASSIFICATION OF ABSTRACT	20. LIMITATION OF ABSTRACT
Unclassified	Unclassified	Unclassified	UL

NSN 7540-01-280-5500

Standard Form 298 (Rev. 2-89)
Prescribed by ANSI Std. Z39-18
298-102